Fabrication and characterization of ZnO:Zn(n^+)/Porous-Silicon/Si(p) heterojunctions for white light emitting diodes

M.A. Vásquez-A[a], G. Romero-Paredes[b], J.A. Andraca-Adame[c] and R. Peña-Sierra[b,*]
[a]*Department of Electronics, INAOE, 72840 Puebla, PUE, México.*
[b]*Department of Electrical Engineering, Solid State Electronic Section (SEES), Centro de Investigación y de Estudios Avanzados del Instituto Politécnico Nacional, México D.F. Phone (55) 5747 377, Fax (55) 5747 3879.*
[c]*Centro de Nanociencias y Micro y Nanotecnologías del Instituto Politécnico Nacional Unidad Profesional "Adolfo López Mateos" calle Luis Enrique Erro S/N, Zacatenco, 07738 México D.F.*

Received 28 September 2015; accepted 16 October 2015

The fabrication and characterization of electroluminescent ZnO:Zn(n^+)/Porous Silicon/Si(p) heterojunctions is presented. Highly conductive ZnO films (ZnO:Zn(n^+)) were produced by applying a temperature annealing at 400°C by 5 min to the ZnO/Zn/ZnO arrange formed by DC sputtering, and the Porous Silicon (PS) films were prepared on p-type (100) Si wafers by anodic etching. The ZnO:Zn(n^+)/PS/Si(p) heterojunction is accomplished by applying a brief temperature annealing stage to the entire ZnO/Zn/ZnO/PS/Si structure to preserve the PS luminescent characteristics. The ZnO:Zn(n^+) films were characterized by X-ray diffraction and Hall-van der Pauw measurements. The PS and ZnO:Zn(n^+) films were also studied by photoluminescence (PL) measurements. The current-voltage characteristics of the heterojunctions showed well defined rectifying behavior with a turn-on voltage of 1.5 V and ideality factor of 5.4. The high ideality factor is explained by the presence of electron tunneling transport aided by energy levels related to the defects at the heterojunction interface and into the PS film. The saturation current and the series resistance of the heterostructure were 4×10^{-7} A/cm^2 and 16 Ω-cm^2, respectively. White color electroluminescence is easily observed at the naked eye when excited with square wave pulses of 8 V and 1 KHz.

Keywords: Porous Silicon; ZnO:Zn(n^+) films; porous silicon-heterostructures; electrical characterization; electroluminescence.

Se reportan los resultados de la fabricación y caracterización de heterouniones ZnO:Zn(n^+)/Silicio Poroso/Si(p). Las películas conductivas de ZnO (ZnO:Zn(n^+)) se obtuvieron aplicando un breve tratamiento térmico a 400°C por 5 min al arreglo ZnO/Zn/ZnO formado por DC sputtering, y las películas de Silicio Poroso (PS) se obtuvieron por anodización electroquímica de obleas de silicio tipo-p con orientación (100). La preparación de las heterouniones de ZnO:Zn(n+)/PS/Si(p) se hizo aplicando el tratamiento térmico a la estructura completa de ZnO/Zn/ZnO/PS/Si para conservar las propiedades luminiscentes del PS. Las características de las películas de ZnO:Zn se determinaron por Difracción de Rayos X y por mediciones eléctricas con el método de Hall-van der Pauw. Las películas de SP y ZnO:Zn(n^+) se caracterizaron también por mediciones de fotoluminiscencia. Las características corriente-voltaje de las heterouniones presentan buen comportamiento rectificante, con voltaje de encendido de 1.5 V y factor de idealidad de 5.4. El factor de idealidad indica que el transporte de carga está controlado por el mecanismo de corriente túnel auxiliado por estados de defecto situados en la interface y en la película de PS. Los valores de la corriente de saturación y la resistencia serie fueron de 4×10^{-7} A/cm^2 y 16 Ω-cm^2, respectivamente. Se produce electroluminiscencia observable a simple vista de color blanco, cuando las heteroestructuras se polarizan con una señal pulsada de 8V de amplitud y frecuencia de 1 KHz.

Descriptores: Silicio poroso; películas de ZnO:Zn(n+); heteroestructuras de silicio poroso; caracterización eléctrica; electroluminiscencia.

PACS: 61.46.-w; 73.63.b; 84.37.+q; 85.60.Jb

1. Introduction

The intense and visible photoluminescence in Porous Silicon (PS) films at 300 K described by L.T. Canhan in 1990 encouraged the development of silicon based electroluminescent devices [1-3]. However up to now there remain important unsolved issues that impede to produce efficient and stable electroluminescent PS based devices. The instability is explained by the huge PS effective surface area leading to the creation of diverse non-radiative centers along the stages involved to build the PS devices. To overcome such difficulties the use of PS functional heterojunctions with distinct materials have been proposed [4-6]. Between them, the use of highly conductive ZnO films result very attractive because they can function as a window layer for their wide band gap and its low chemical reactivity with the PS providing a passivating film. Hence, the realization of ZnO/PS heterojunctions offers the possibility to develop electroluminescent devices capable to produce visible electroluminescence (EL). To reach this objective the fabrication process must exclude high temperature processing stages to keep unchanged the PS photoluminescence response. In a previous work we reported a method to produce highly conductive ZnO:Zn(n^+) thin films comprising a brief temperature annealing stage at 400°C by 5 min to the ZnO/Zn/ZnO arrange grown by DC sputtering [7]; this procedure can be advantageously used to produce functional ZnO:Zn(n^+)/PS-heterojunctions while keeping the PS luminescent properties.

In this work a complete procedure to build electroluminescent ZnO:Zn(n^+)/PS/Si(p) heterojunctions is reported,

their structural and electrical characterization is also described. The heterostructures produce white light when biased under the DC pulse biased regime.

2. Experimental procedure

The procedure to fabricate the ZnO:Zn(n^+)/PS/Si(p) heterojunctions comprises four stages. The first one is the formation of PS films on p-type Si crystalline wafers; the second stage is the deposition of the (ZnO/Zn/ZnO)/PS/Si(p) multilayer; the third is an annealing stage applied to the entire structure at 400°C by 5 min in inert N_2 gas, to produce highly conductive ZnO:Zn(n^+) films over PS/Si(p) according to the process reported in [7] and to kept without change the PS luminescent response; finally ohmic contacts are fabricated on each side of the structure to electrically characterize them. Control samples of ZnO:Zn(n^+) were grown on corning glass substrates to verify their physicochemical properties.

The PS films were prepared on 1-5 Ω-cm p-type (100) Si wafers by anodic etching using the home-made all-Teflon electrochemical cell sketched in the Fig. 1, the details of the entire procedure was reported before [8]. The etching process was carried out in a Hydrofluoric Acid (48%):Propanol:H_2O (1:2:1) electrolyte, with a current density of 15 mA cm^{-2} for 5 min. After the anodization stage the PS films were rinsed with ethanol for 2 min and dried under N_2 gas flow. The used experimental conditions produce highly resistive PS films of ∼1.2 μm in thickness as measured with the aid of Scanning Electron Microscope (SEM) on cleavage PS/Si(p) samples, as described in [9].

Highly conductive ZnO:Zn(n^+) films are produced in two stages. In the first one the ZnO/Zn/ZnO multilayer is deposited by DC reactive sputtering in a controlled Ar/O_2 gas mixture using Zinc targets (99.99%) as was described elsewhere [7]. The ZnO and Zn films were deposited at a work pressure of 1 Pa in the chamber by fixing the Ar inlet at a flow of 7 sccm. The Zn metallic films were deposited with a power of 25 W in Ar atmosphere; films of 10 nm in thickness were produced for a deposition period of 10 sec. Highly resistive oxygen-rich ZnO was deposited with a power of 100 W using an Ar/O_2 flow ratio of 80/20%; for a deposition period of 30 min films of 31 nm in thickness were produced. The full thickness of the ZnO/Zn/ZnO multilayer structure was of ∼75 nm. In the final stage the ZnO/Zn/ZnO arrange is annealed at 400°C in inert N_2 gas by 5 min to produce highly conductive ZnO:Zn(n^+) films [7].

The PS and ZnO:Zn(n^+) films were studied by PL measurements. The structural characteristics of ZnO:Zn(n^+) films were studied by X-ray diffraction (XRD) using a X'Pert PRO PANalytical diffractometer. CuKα radiation (1.5406Å) was used at 45 kV and 40 mA. The electrical properties of the ZnO based films were measured by the Hall-van der Pauw method in a magnetic field of 0.55 Tesla. To measure the heterojunction electrical characteristics ohmic contacts were deposited in a vacuum evaporation system; the high conductivity of the ZnO:Zn(n^+) makes simply the formation of electrical contacts but a small In dot of less than a 0.5 mm in diameter was used to protect the sample surface, on the rear side of the p-type silicon substrate a continuous aluminum film forms the opposite electrical contact. The current-voltage (I-V) characteristics of the ZnO:Zn(n^+)/PS/Si(p) heterostructures were measured with a Keithley Semiconductor Characterization System, model 4200-SCS.

3. Results and Discussion

PL spectra of PS and ZnO:Zn(n^+) films taken at room temperature are shown in Fig. 2. The PL spectra of the as-prepared PS is an intense Gaussian-like shape line with its peak located at 657 nm with a full width at half maximum (FWHM) of 140 nm. The PL spectra characteristics depend on the used anodization parameters and possess similar characteristics to those frequently reported in the literature [9,10]. PL spectra were also taken on thermal annealed PS control samples to verify the luminescence response; undetectable

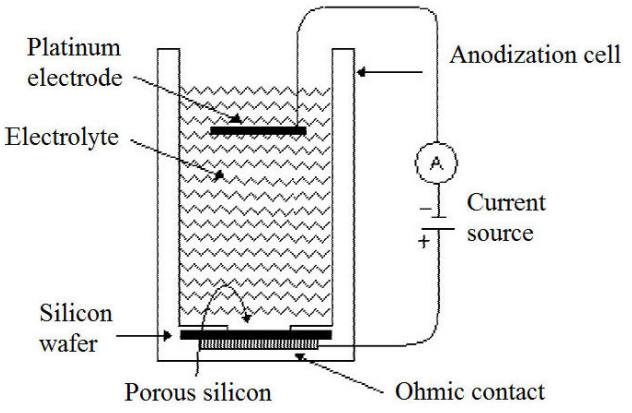

FIGURE 1. Schematic diagram of all Teflon electrochemical cell used to produce the porous silicon films.

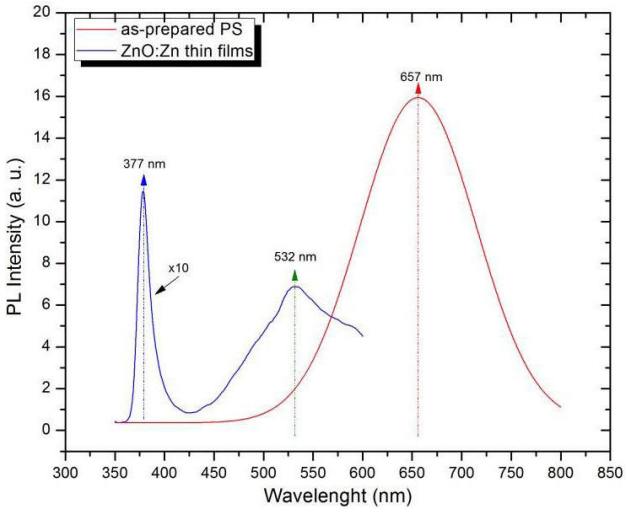

FIGURE 2. Room temperature PL spectrum of; a) an as-prepared PS film and b) a ZnO:Zn(n^+) thin film.

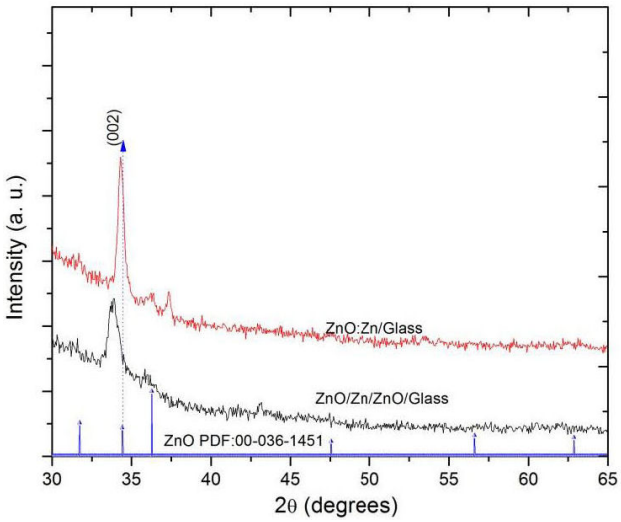

FIGURE 3. XRD patterns of the as-deposited ZnO/Zn/ZnO/Glass structure and the ZnO:Zn(n^+) films.

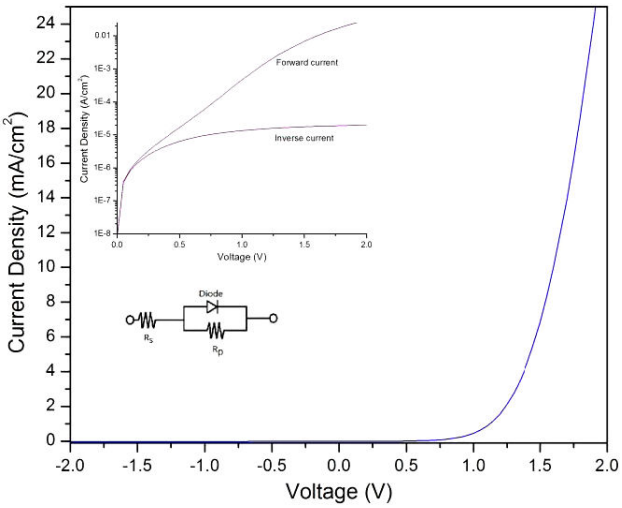

FIGURE 4. I-V characteristics of the ZnO:Zn(n^+)/PS/Si(p) heterojunction. The insets are a semi-log I-V characteristic and an equivalent electrical circuit.

changes in the PL signal were observed in samples annealed at the same conditions as the processed ones with respect to fresh PS films.

The PL spectrum of ZnO:Zn(n^+) films is formed by a strong ultraviolet (UV) emission at around 377 nm with an intense deep-level band centered at 532 nm [11,12]. The UV line at 377 nm is characteristic of the ZnO films and the deep-level band matches to the bands produced by intrinsic defects in ZnO [13-15].

Figure 3 shows the XRD patterns for both the as-deposited ZnO/Zn/ZnO structure and the ZnO:Zn(n^+) films formed on glass substrates. The ZnO:Zn(n^+) films resulted nanocrystalline with the dominant hexagonal (002) planes parallel to substrate surface; crystallites size are $\sim$19 nm as estimated with the Scherrer equation [16]. The as-deposited ZnO/Zn/ZnO structure is under tensile stress but this was relieved after the short annealing stage at 400°C by 5 min. As a reference the diffraction lines of the ZnO powder from the PDF database ICDD # 00-036-1451 is included.

The electrical properties of ZnO:Zn(n^+) films deposited on glass substrates shown values similar as those reported before [7]. It must be pointed out that the as-grown ZnO films resulted highly resistive and their electrical properties could not be measured with our laboratory facilities. In a similar way the as-grown ZnO/Zn/ZnO arranges resulted highly resistive, however with the short annealing stage at 400°C by 5 min highly conductive ZnO:Zn(n^+) films were produced. The electrical resistivity and carrier mobility of the ZnO:Zn(n^+) films were 1×10^{-2} Ω-cm and 12 cm^2/V-s respectively, with an electron concentration of 4×10^{19} cm^{-3}. The sharp decrease in the resistivity can be explained by the formation of Zn interstitials sites (Zni) into the contiguous ZnO films. Taking into account these results we can argue that the use of the ZnO/Zn/ZnO multilayer is a straightforward method to generate zinc interstitial sites. Furthermore, the nanocrystalline nature of the ZnO films helps the Zn diffusion to the neighboring ZnO layers producing Zni sites. With this procedure the electrical properties of the ZnO:Zn(n^+) films can be controlled within manageable periods of time.

Figure 4 shows the linear I-V characteristics of the ZnO:Zn(n^+)/PS/Si(p) heterostructure. The measured forward current density was 23 mA/cm^2 at 1.7 V, with a turn on voltage of 1.5 V. From the analysis of the I-V characteristics it is possible to propose the electrical circuit shown in the inset of the Fig. 4. The electrical parameters for the heterostructure were: ideality factor 5.4, series resistance 16.0 Ω-cm^2, shunt resistance 32.2×10^5 Ω-cm^2 and 3.96×10^{-7} A/cm^2 for the saturation current. The high values of the ideality factor, clearly noticeable over three current cycles, can be explained by the tunneling mechanism aided by defective energy levels at the PS surface films and the interfacial intrinsic states.

Although the saturation current in the heterostructures is relatively large, the measured values are lower than the ones usually reported [17]. Otherwise, the large series resistance is mainly due to the high resistivity of the PS films and the interfacial defects [18,19]. In spite of the relatively low values of the measured series resistance several deleterious effects were observed during the device operation, for example a continuous increase in the sample temperature was produced when the structure was DC biased. The mechanisms producing these effects are linked to non-radiative recombination at the interface ZnO:Zn(n^+)/PS by the complexity of the PS structure. As was discussed in a previous work [20] the carrier transport in the PS layers is mainly controlled by the space charge limiting (SCL) mechanism.

A significant issue that has not been sufficiently discussed in the literature is the effect produced by the presence of charge trapping centers distributed in the PS films. These centers act reducing the radiative recombination and modify the devices time response. Taking into account the distinct

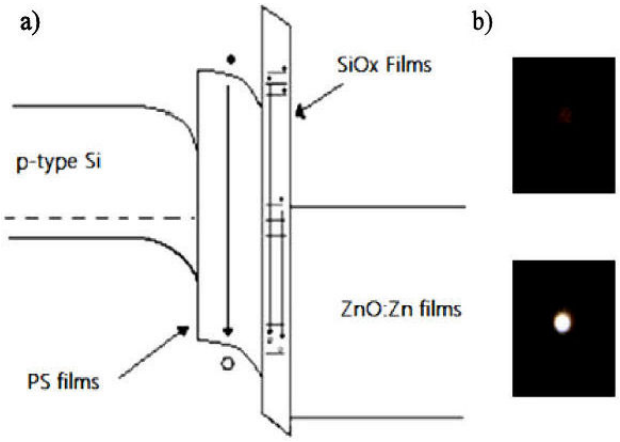

FIGURE 5. a) Energy band diagram in equilibrium of the ZnO:Zn(n^+)/PS/Si(p) heterostructure, b) photographic images of the electroluminescence produced by the pulsed biasing mode.

effects in the PS based heterostructures, an energy band diagram in equilibrium is illustrated in Fig. 5a) for the realized heterojunction. According to the heterostructure I-V characteristics several current controlling mechanisms merge in the structure by the complex nature of the PS film and the PS/ZnO:Zn interface [21,22]. A simplified scheme of the energy bands, including the possible defect states located at the heterojunction interface and into the PS films is illustrated in the Fig. 5a).

To reduce the heating effects due to the high series resistance the structures can be biased with AC pulses; this biasing mode helps reducing degradation effects, modifying the charge trapping events, and helps in reducing the electrical instability effects. In this line the ZnO:Zn(n^+)/PS/Si(p) heterostructures were biased with square wave pulses at 1 KHz to excite the EL response. In the Fig. 5b) photographs of a turn-on device are included; the white color is produced when biasing with pulses of 8 V and the color change to red with pulses of 5 V. The EL intensity is relatively weak but a uniformly shined area is produced, in contrast with our previous report for Metal-PS structures where the EL is only produced at the borderline of the metal contact [3]. The changes in the color of the EL response could be explained by the subbands filling process within the PS nano-crystallites. This is possible because there is a lot of trapping centers into the PS films that change their occupation conditions when the bias is changed. The variation on the defect states charge condition driven by the electrical field allows the PS films subbands filling then producing color changes. In general, the pulse bias modes modify the carrier injection process into the heterostructure with the consequently change in the radiative recombination regime. As our recording system to measure the EL response requires several minutes, in this stage of the work was difficult to take reliable excited EL spectra. Additional work is in course to gain control on the ways to increase the heterostructure stability response and to increase the EL efficiency in our devices.

4. Conclusions

A complete and functional procedure to fabricate electroluminescent ZnO:Zn(n+)/PS/Si(p) heterojunctions was developed. The heterojunctions were fabricated by depositing highly conductive ZnO:Zn(n^+) layers onto PS films, including an annealing stage at 400°C in N_2 by 5 minutes to conserve the PL response without change. This novel method involves the addition of a highly conductive ZnO based films of controllable and reproducible properties. The low temperature annealing process used for the heterostructure fabrication conserves without change the PS photoluminescence response. The DC characterization of the ZnO:Zn/PS/Si(p) structure showed a well defined rectifying behavior with practical saturation current. The ideality factor of 5.4 is explained by the tunneling current mechanism aided by the mid-gap energy levels at the heterojunction interface and into the PS film. The EL response of the ZnO:Zn(n^+)/PS/Si structures produced by the bias pulsed mode is visible to the naked eye, the emission is white but color changes are produced as the pulse amplitude is varied.

Acknowledgments

We want to acknowledge to M. Sc. Miguel Galván Arellano and M. Sc. Adolfo Tavira Fuentes for his valuable support in the I-V and X-ray diffraction measurements, respectively.

Part of this work was supported by the Instituto de Ciencias y Tecnología del Distrito Federal under the contact "Proyecto ICyT-DF 326/11".

1. L.T. Canham, *Appl. Phys. Lett.* **57** (1990) 1046.
2. B, Min, W.M. Kyung; Y. Jangyeol; K. Gyu-Tae; S. Ha. Jeong, *J. Appl. Phys*. **113** (2013) 084310.
3. G. Romero-Paredes R., R. Peña-Sierra and G. Castillo Cabrera, *Rev. Mex. Fis.* **48** (2002) 92.
4. V.S. Vidhya *et al*., *J. Alloys and Compounds* **509** (2011) 2842.
5. C-F Wang, B. Hub, H.H. Yia, and W.B. Lia, *Optics and Spectroscopy*, **116** (2014) 427.
6. K-J. Moon, T.I. Lee, W. Lee and J-M. Myoung, *Nanoscale*, **6** (2014) 3611.
7. M. A.Vásquez-A., O., Goiz; R. Baca-Arroyo, J. A. Andraca-Adame, G. Romero-Paredes, R. Peña-Sierra, *Journal of Nanoscience and Nanotechnology* **12** (2012) 9234
8. M. A. Vásquez-A, G. Águila Rodríguez, G. García-Salgado, G. Romero-Paredes and R. Peña-Sierra, *Rev. Mex. Fis.* **53** (2007) 431.

9. F. Ruiz *et al*., *J. Vac. Sci. Technol. A* **12** (1994) 2565.
10. L. Pavesi, M. Ceschini, F. Rossi, *J. Lumin* **57** (1993) 131.
11. J. Petersen *et al*., *J. Appl. Phys.* **104** (2008) 113539.
12. Ch. H. Ahn, Y.Y. Kim, D. Ch. Kim, S. K.R. Mohanta, and H.K. Cho, *J. Appl. Phys.* **105** (2009) 013502 .
13. M-K. Lee and H-F. Tu, *J. Appl. Phys.* **101** (2007) 126103.
14. B. Lin, Zh. Fu, and Y. Jia, *Appl. Phys. Lett.* **79** (2001) 943.
15. M.A. Reshchikov, J.Q. Xie, B. Hertog, and A. Osinsky, *J. Appl. Phys.* **103** (2008) 103514.
16. B.D. Cullity, *Elements of X-Ray Diffraction*, Addison-Wesley, Massachusetts **356** (1978).
17. H.A. Hadi and I.H. Hashim, *Journal of Electron Devices* **20** (2014) 1701.
18. S. Lazarouk *et al*., *Appl. Phys. Lett.* **68** (1996) 1646.
19. R.G. Singh, F. Singh, D. Kanjilal, V. Agarwal and R.M. Mehra, *J. Phys. D: Appl. Phys. 42* (2009) 062002.
20. M. A. Vásquez-A, G. Romero-Paredes and R. Peña-Sierra, *Superficies y Vacío* **24** (2011) 5.
21. A. Gokarna, N.R. Pavaskar, S.D. Sathaye, V. Ganesan, and S.V. Bhoraskar, *J. Appl. Phys.* **72** (1992) 5401.
22. Y. Ding, X. Y. Kong and Z. L. Wang, *J. Appl. Phys.* **95** (2004) 306.